Phage-display derived single-chain fragment variable (scFv) antibodies recognizing conformational epitopes of Escherichia coli heat-labile enterotoxin B-subunit

Wen Yuan Chung[1,7], Markus Sack[2], Rachel Carter[3], Holger Spiegel[4], Rainer Fischer[2,4], Timothy R. Hirst[5], Neil A. Williams[6], Roger F.L. James[7*]

[1]Royal College of Surgeons, Department of Surgery, Connolly Hospital, Blanchardstown, D15, Ireland,
[2]Department of Molecular Biotechnology, RWTH Aachen University, 52074 Aachen, Germany,
[3]CRUK Clinical Centre, Southampton, S016 6YD, UK,
[4]Fraunhofer IME, Institute for Molecular Biology and Applied Ecology, 52074 Aachen, Germany,
[5]Cellular Microbiology, John Curtin School of Medical Research, Australian National University, Canberra, ACT 0200, Australia,
[6]Department of Cell and Molecular Medicine, University of Bristol, Bristol BS8 1TD and
[7]Department of Infection, Immunity and Inflammation, University of Leicester, Leicester, LE1 9HN, UK.

*Corresponding author: Dr. Roger F.L. James, Department of Infection, Immunity and Inflammation, University of Leicester, Maurice Shock Building, University Road, Leicester LE1 9HN, UK. Phone: 44 (0)116 2231406 44(0)116 2525033; Fax: 0116 2525035; Email:rj1@le.ac.uk

Abbreviations: *E.coli*, *Escherichia coli*; scFv, single-chain Fv antibody fragment; ELISA, enzyme-linked immunosorbent assay; G_{M1}, monoganglioside-G_{M1} (Galβ-3GalNacβ1-(neu5Acα2-3)-4Galβ1-4Glcβ1-cer); Etx, heat-labile enterotoxin; $EtxB_5$, heat-labile enterotoxin B pentamer; $EtxB_1$, heat-labile enterotoxin B subunit monomer; Ctx, cholera toxin; mAb, monoclonal antibody; SDS-PAGE, sodium dodecylsulphate polyacrylamide gel electrophoresis; CDR, complementary determining region; V_H, heavy chain of an antibody; V_L, light chain of an antibody; DTT, dithiotreitol; PBS, phosphate buffer saline; MBP, myelin basic protein.

Previously we have described studies on *in vitro* pentamer assembly of *Escherichia coli* (E. coli) derived heat-labile enterotoxin B subunit (EtxB) using conventional monoclonal antibodies (Amin *et al*. JBC 1995: 270, 20143-50 and Chung *et al*. JBC 2006: 281, 39465-70). To extend these studies further we have used phage-display to select single-chain Fragment variable (scFv) antibodies against different forms of the B-subunit. Two clones exhibiting strong and differential binding were chosen for detailed characterization. A comprehensive sequence analysis was performed to assign the framework and complementary-determining regions and a nonsense mutation present in one of these (scFv-B1.3.9) was

corrected. Binding analysis showed that scFv-B1.3.9 bound in ELISA to both heat-denatured monomeric B-subunits ($EtxB_1$) and also displayed cross-reactivity towards pentameric EtxB ($EtxB_5$), although there was no reactivity towards monoganglioside (G_{M1}) captured $EtxB_5$. Another antibody (scFv-B5.2.14) had a different reactivity profile and, in ELISA, bound only to $EtxB_5$ but not to $EtxB_1$ or to $EtxB_5$ captured via $G_{M1.}$ Surprisingly, in competition experiments, the assembled pentameric B-subunit inhibited binding of scFv-B5.2.14 to immobilized $EtxB_5$ only weakly, whereas reduced, but not oxidized, monomeric $EtxB_1$ was an efficient competitor. These results clearly demonstrate that B1.3.9 and B5.2.14 have different specificities for cryptic epitopes not accessible in the fully assembled G_{M1} bound pentameric form of EtxB.

Taken together our results show that we were able to successfully isolate and characterize recombinant scFvs that differentially recognize diverse denatured forms or assembly intermediates of the heat-labile enterotoxin B subunit of *E. coli*.

KEYWORDS

EtxB, epitope, protein assembly, differential recognition, phage display, recombinant antibodies, scFvs

Heat-labile enterotoxin (Etx) produced by certain strains of *E. coli* is a major virulence factor related to cholera toxin (Ctx) produced by *Vibrio cholera* and results in diarrhoeal disease in humans and animals (Hirst, 1995; Echeverria *et al.*, 1985). Heat-labile enterotoxin consists of 5 identical B-subunits (Mr = 12,000), which *in vivo* naturally assemble into a stable pentameric structure with an A-subunit (Mr = 28,000), which has ADP-ribosyl transferase activity (Holmgren *et al.*, 1975; Fishman *et al.*, 1978; Fishman *et al.*, 1980). The B-subunit pentamer of Etx ($EtxB_5$) specifically recognizes, and has a high affinity for, the oligosaccharide portion of G_{M1} on the surface of intestinal cells and acts to deliver the A-subunit

where it catalyses ADP-ribosylation of the signal transduction protein G_s-α. By effectively blocking deactivation of G_s-α intracellular levels of cAMP rise, leading to fluid and Cl^- loss from the cells and thus severe diarrhoea (Kuziemko *et al.*, 1996; Turnbull *et al.*, 2004).

In addition to their roles as mediators of diarrhoeal disease, Etx and Ctx have long been known to be potent mucosal immunogens and, when co-administered with other antigens, can give rise to strong tolerogenic responses (Weiner, 1997). In addition, it has been shown that recombinant preparations of $EtxB_5$ affect immunoregulatory processes and lead to the suppression of inflammatory responses (Shevach, 2000). The enterotoxins Etx and Ctx are highly related showing 80% sequence identity and stimulate strong mucosal immunity both to themselves and to co-administered antigens (Yamamoto *et al.*, 1987; Wilson *et al.*, 1991; Takahashi *et al.*, 1996). The ability of EtxB and CtxB to enhance T_{H2} and suppress T_{H1} inflammatory responses in an antigen-specific manner has been subject to intensive research, particularly in relation to the treatment of autoimmune disease (Williams *et al.*, 1999; Sobel *et al.*, 1998; Luross *et al.*, 2002). It was initially thought that the adjuvant properties of EtxB were dependent on receptor binding activity as a non-binding point mutant of EtxB (G33D), lost all immunomodulatory activity. However, the CtxB mutant, CtxB (H57A) was shown to retain the ability to bind to G_{M1} but was unable to act as an immunomodulator (Truitt *et al.*, 1998; Williams *et al.*, 1999; Aman *et al.*, 2001; Fraser *et al.*, 2003). It is now theorized that structural alterations in CtxB (H57A), while not preventing binding to G_{M1}, may preclude interactions with additional co-receptors required for signaling (Fraser *et al.*, 2003). Therefore, ganglioside recognition alone, while necessary to achieve high-affinity binding to cell surfaces, may not be sufficient to mediate the immunomodulatory effects of the B subunits.

Previously we reported on the generation and characterization of mAbs specific for $EtxB_5$ (LDS16) and $EtxB_1$ (LDS47) and showed that

these could be used to study pentamer assembly *in vitro* and this has led us to propose a model describing the processes of pentamer assembly (Lesieur, 2002). However, investigating *in vivo* toxin assembly and transport to the periplasmic space using mAb probes is not possible using conventional monoclonal antibodies. In this study we have selected scFvs that specifically react with intermediate forms of EtxB with the potential to be used to study pentamer assembly *in vivo*.

EXPERIMENTAL PROCEDURES

Phage display library and phage rescue – Antibodies against different forms of EtxB were selected from the semi-synthetic scFv phage display library (a generous gift from Dr. Andrew Griffiths, MRC, Cambridge, UK). The V_H and V_L regions were re-cloned from the lox library vectors into the phagemid pHEN2 (Griffiths *et al.*, 1994) where the recombinant scFv genes are flanked by *Sfi*I and *Not*I sites. Rescue of the library was performed as recommended (Griffiths *et al.*, 1994). Briefly, 10^{10} CFU of the Griffin.1 library in bacterial strain TG1 were inoculated into 2xTY medium containing 100 μg/ml ampicillin and 1% glucose. Cells were incubated at 37°C until the OD_{600} reached 0.5. Then 25 ml of this culture was infected with 10^{10} PFU of VCS-M13 helper phage and incubated for 30 min at 37°C. The infected cells were collected by centrifugation for 10 min at 2,500 *g* and resuspended in 300 ml of 2xTY containing 100 μg/ml ampicillin and 25 μg/ml kanamycin. Subsequently, the bacteria were cultured overnight at 37°C with slow rotation (200 rpm). After centrifugation for 30 min at 2,500 *g* the supernatant was collected and phages were precipitated twice with 20% polyethylene glycol 6,000 and 2.5 M NaCl. The phage pellet was resuspended in PBS to a final titer of $10^{12\text{-}13}$ PFU/ml.

Biopanning – Nunc immunotubes (maxisorp®) were coated overnight with 4 ml of monomeric and pentameric EtxB (10 μg/ml) at room temperature in 50 mM carbonate buffer, pH 9.6. After washing three times with PBS the tubes

were blocked with 2% milk in PBS and incubated at 37°C for 2 h. Phages (10^{12} PFU) were diluted into 4 ml of 2% dried milk powder in PBS and were incubated for 30 min at room temperature with slight agitation followed by 90 min at room temperature without agitation. The tubes were thoroughly washed ten times with PBS containing 0.1% Tween-20, and then ten times with PBS. Phages were eluted by 10 min incubation with 1 ml of 100 mM triethylamine under slight agitation. The eluted phages were then immediately neutralized with 0.2 ml of 1 M Tris pH 7.4. The immuno-tubes were rinsed with 0.2 ml 1 M Tris pH 7.4 to neutralize the remaining phages and 0.75 ml of the eluted phages were added to 9.25 ml of an exponentially growing TG1 culture (OD_{600} of 0.6 to 0.8). In addition, 4 ml of this culture were added to the immuno-tube to collect any remaining phages. Both cultures were incubated for 30 minutes at 37°C in a water bath without shaking to allow infection. The cultures were then pooled and serial dilutions were plated on TYE containing 100 μg/ml ampicillin and 1% glucose for titer determination. The remaining culture was centrifuged at 3,300 *g* for 10 minutes and resuspended in 1ml of 2xTY and plated on a large Nunc Bio-Assay dish of TYE containing 100 μg/ml ampicillin and 1 % glucose. After overnight incubation at 30°C, 5-6 ml of 2xTY and 15% glycerol was added to the Bio-Assay dish and the cells were suspended with a glass spreader. The bacteria were then incubated in 2xTY medium containing ampicillin (100 μg/ml) and 1% glucose at 37°C with shaking until the OD_{600} reached 0.5. Subsequent selection of primarily purified phages was also done using Nunc immunotubes (maxisorp®) coated overnight with 4 ml of monomeric and pentameric EtxB (10 μg/ml) at room temperature in 50 mM carbonate buffer, pH 9.6.

Preparation of monoclonal phages – Monoclonal phages were prepared by inoculating individual colonies from the TYE plates into 100 μl of 2xTY containing 100 μg/ml ampicillin and 1% glucose in 96 well plates and grown at 37°C overnight with shaking at 300 rpm. 2 μl of

each well from this plate was transferred to a second 96-well plate containing 200 μl of 2xTY with 100 μg/ml ampicillin and 1% glucose per well and incubated at 37°C for 1 h. Then 25 μl 2xTY containing 100 μg/ml ampicillin, 1% glucose and 10^9 PFU VCS-M13 helper phage was added to each well. After 90 min incubation at 37°C the plate was spun at (10 min at 1,800 *g*), the pellet was resuspended in 200 μl 2xTY containing 100 μg/ml ampicillin and 50 μg/ml kanamycin and incubated overnight at 30°C with shaking. The plate was spun (10 min at 1,800 *g*) and 100 μl of the supernatant was used in phage-ELISA.

Enzyme-linked immunosorbent assays – The production and purification of recombinant pentameric B-subunit ($EtxB_5$) has been described previously (Amin *et al*., 1995).. For the G_{M1}- EtxB ELISA, microtiter plates (Immulon 1, Dynatech) were coated with G_{M1}-ganglioside (0.2μg/ml) overnight and 0.2μg/ml $EtxB_5$ in PBS was added 1hr before the assay. Plates were blocked with 1% bovine serum albumin (BSA) and antibody binding to G_{M1} captured EtxB was detected using a goat anti-mouse-horse radish peroxidase conjugate (Jackson Immunoresearch Laboratories).

For direct binding experiments not involving the capture of $EtxB_5$ by G_{M1}. $EtxB_5$ and $EtxB_1$ ($EtxB_5$ boiled for 5min) were coated directly onto the plates in PBS for 1hr at room temperature and blocked with BSA buffer as above. To confirm that plates were coated with $EtxB_5$ or $EtxB_1$ we used the monoclonal antibodies against pentamer (LDS16) and monomer (LDS47) as controls (Chung et al., 2006). An scFv against MBP was also used as an internal positive control for the detection system in ELISA (kindly provided by Dr. K. Gough, Department of Biology, University of Leicester (Gough *et al*., 1999)) although data for this is not shown for reasons of clarity. For the phage-ELISA, 10 μl (about 10^{10} PFU) of poly-ethylene glycol-precipitated polyclonal phage antibodies from each round of selection (made up to 100 μl with blocking buffer) or 100 μl of culture supernatant of super-infected TG1 cells containing monoclonal phage antibodies was applied to the coated and blocked plates and incubated for

90 min at room temperature. Plates were washed three times with PBS containing 0.05% Tween-20 and three times with PBS. Phages were detected by using the Detection Module Recombinant Phage Antibody System (Pharmacia, Uppsala, Sweden) according to the manufacturer's recommendations.

To test for secreted scFvs, *E. coli* supernatants were applied to the coated and blocked plates and incubated for 1.5 h. Then the anti-c-myc monoclonal antibody (9E10, 1/50 dilution of hybridoma supernatant) was added and incubated for 1.5 h followed by 1 h incubation with goat anti-mouse IgG conjugated to horseradish peroxidase (Jackson Immunoresearch Laboratories). The substrate reaction was carried out for 1 h in the dark. The reaction was stopped by addition of 1 M H_2SO_4 and the absorbance was measured at 450 nm.

Inhibition of scFv-B5.2.14 binding was analyzed by first incubating $EtxB_1$/$EtxB_5$ with either B5.2.14 (*E. coli* supernatant containing the secreted scFv) or LDS16 (diluted 1/50 in PBS) for 1 h at room temperature before adding to the ELISA plates directly coated with $EtxB_5$ or G_{M1}-captured $EtxB_5$ and subsequently blocked with 1% milk powder in PBS. The inhibition was calculated using:

$$I = 1 - \frac{OD\,(competitor)}{OD\,(no\ competitor)}$$

For quantification of the amount of $EtxB_5$ bound to the ELISA plates for each test sample, optical density readings corresponding to dilutions located on the linear part of the curve were compared with the dilution of an $EtxB_5$ standard (1 μg/ml, diluted 2-fold), giving the same optical density reading.

Correction of the scFv-B1.3.9 gene – The nonsense mutation identified in the V_H region of scFv-B1.3.9 was corrected by SOE-PCR using the primers pSOEp1 (5' AAA TTC CAA GAC AGA GTC ACC ATT ACC AG 3'), pSOEp2 (5' GGT GAC TCT GTC TTG GAA TTT CTG TGC GTA GTT 3'), pGSRp3 (5' TCC GCC TGA ACC GCC TCC AC 3') and LMB3 (5' CAG GAA ACA GCT ATG AC 3'). The SOE-PCR product was gel-

purified and digested with *Sfi*I and *Xho*I. The corresponding region of pHEN2-scFv-B1.3.9 as excised and the gel-purified vector-fragment (V-F) was ligated to the digested SOE-PCR product. The ligated product was transformed into electro-competent XL1-blue cells. Ampicillin-resistant colonies were isolated for further analysis.

Structural analysis – The variable regions of B1.3.9 and B5.2.14 were sequenced and their deduced amino-acid sequences were analyzed by aligning them to the human germline sequences (http://imgt.cines.fr/). The complementary determining regions were assigned according to Chothia (Chothia *et al.*, 1992). 3D models of the scFvs were generated by homology-based modeling using the SWISS-model and WAM (Chothia *et al.*, 1992). Graphic representations of the 3D molecular features were generated with the Swiss-PdbViewer v3.7 software package (Guex *et al.*, 1997) using previously published structures of $CtxB_5$ (Merritt *et al.*, 1997) and $EtxB_5$ (Sixma *et al.*, 1992). Electrostatic molecular surface potentials were generated using the eF-site (http://ef-site.hgc.jp/)

Expression of soluble scFv – *E. coli* HB2151 was infected with individual phages for 30 min at 37°C and then plated onto TYE plates containing 100 μg/ml ampicillin and incubated overnight at 37°C. Single colonies were inoculated in 2xTY medium (16 g/L tryptone, 10 g/L yeast extract and 5 g/L NaCl) containing 100 μg/ml ampicillin and 1% glucose. scFv expression was induced with 1 mM isopropyl β-D-thiogalactoside (IPTG) when the cultures reached an $OD_{600} = 0.9$. The cultures were further incubated overnight at 30°C and the culture supernatants containing the secreted scFvs were collected by centrifugation at 3,000 rpm for 15 min for subsequent analysis. Periplasmic extracts were prepared by resuspending the bacterial pellet in 10 ml of ice-cold PBS, pH 7.2 containing polymyxi B sulphate (1,000 units/ml) and incubated on ice for 15 min. Samples were centrifuged for 10 min at 4°C at 3,000 rpm and 100 µl of the supernatants were used for ELISA.

SDS-polyacrylamide Gel Electrophoresis and Western blot-

EtxB5 (8μg), boiled (5min) EtxB5 (EtxB1 – 8□g) and boiled/reduced (in 30mM dithiothreitol) were loaded into SDS-polyacrylamide 14% (w/v) gels for electrophoresis on a Bio-Rad Protean II system. After SDS-PAGE, gels were transferred to nitrocellulose paper with transfer buffer in a Bio-Rad Trans-Blot apparatus for 45 min to permit efficient transfer. Non-specific binding sites were blocked overnight in PBS containing 5% (w/v) Marvel. Blots were washed in PBS containing 0.05% v/v Tween 20 (PBS-T) for 3 x 10min with agitation. B5.2.14 supernatant (approximately 2□g/ml) was used neat for 1h at room temperature with agitation. Blots was washed as previously and incubated with goat anti-mouse IgG conjugated to horseradish peroxidase diluted 1:2000 for 1h. The blots were then washed and developed with an enhanced chemiluminescence system (ECL, Amersham) for 10min.

RESULTS

Selection of phage-displayed scFvs – The Griffin.1 human scFv library was expanded and the phagemids selected by solid phase panning using antigen directly coated to test tubes (immuno-tubes). After initial panning, antigen-binding phages were collected and expanded following re-infection of TG1 bacterial cells. This cycle of selection and expansion was repeated 3 times following selection for phagemids binding to either $EtxB_1$ or $EtxB_5$. Resulting enrichment was assessed using ELISA against plates coated with either $EtxB_1$ or $EtxB_5$ (Figure 1). $EtxB_5$ specificities were in greater abundance in the library and by the third round the majority of colonies tested had reactivity against $EtxB_5$. It was clear that the library had less reactivity against $EtxB_1$ and even after 3 rounds of selection against $EtxB_1$ there was markedly less reactivity seen in the isolated phages (Figure 1).

Analysis of selected monoclonal phages – The clones displaying the highest reactivities were then transfected into *E. coli* TG1 cells for scale up to confirm the antigen-binding properties and follwing the expansion of the 3 $EtxB_1$ selected clones in TG1 cells only phage-displayed B1.3.9 showed consistent reactivity in ELISA (Figure 2A). In terms of specificity B1.3.9 also showed reactivity against $EtxB_5$ coated directly to plastic (Figure 2A). However, following transfection of the phagemid into permissive HB2151 bacterial cells, no soluble scFv was present (Figure 2B) (summarized in Table 1). This is discussed later in relation to the sequence analysis.

Two of the 4 phagemid colonies expanded in TG1 cells from the selected $EtxB_5$ panning showed consistent results in ELISA (Figure 2A) and both B5.2.11 and B5.2.14 both gave a higher ELISA signal for $EtxB_5$ over $EtxB_1$. However, only the $EtxB_5$ specific scFv (B5.2.14) was secreted following transfection into HB2151 cells (Figure 2B).

Sequence analysis of B.1.3.9 and B5.2.14 scFv – The inserts of scFvs that were specific for $EtxB_1$ or $EtxB_5$ (B1.3.9 and B5.2.14) were sequenced to assess their germline alignment specificities compared to the published V-BASE directory. The phage display library was generated from human VH, Vλ and Vκ germline exons and its generation and composition has been described and analyzed in great detail (Tomlinson *et al.*, 1992; Nissim *et al.*, 1994). A detailed comparison with the identified scFv-clones was therefore done to identify unusual sequence features or artifacts that may have been acquired during the course of the experiments. We therefore determined the DNA sequences of scFv-B1.3.9 and scFv-B5.2.14 (Figure 3) and identified the corresponding germline exons.

The VL of ScFv-B5.2.14 belongs to the Vλ-I subgroup and has highest homology with germline segment DP-L3. There is one single nucleotide change leading to a conservative $Gly^{95b} \rightarrow Ala^{95b}$ mutation located in the CDR-L3. The VH of scFv-B5.2.14 belongs to the VH-I

subgroup and shows closest homology to the germline segment DP-14. There is also one conservative mutation leading to a $Trp^{103} \rightarrow Leu^{103}$ change. Trp^{103} is a very strongly conserved residue and is found in all 6 germline segments of the joining element. Both observed mutations are exactly at the junctions where the 0-3 and 4-12 amino acid long random insertions have been made (Nissim *et al.*, 1994). This suggests that these mutations have likely resulted from the initial generation of the recombinant antibody genes and were not acquired during panning and selection.

The VL of scFv-B1.3.9 belongs to the Vλ-III subgroup showing highest homology to the germline segment DP-L16 (Figure 3). There are three amino acid changes, all of which are not critical in terms of structural aspects. The $Thr^{5} \rightarrow Ile^{5}$ change is located in framework-1 and is a surface exposed residue. The $Asn^{95a} \rightarrow Thr^{95a}$ and $His^{95b} \rightarrow Val^{95b}$ changes are located in CDR-L3 and are likely part of the paratope of scFv-B1.3.9. These residues are also located at the junction where the 0-3 amino acid long random insertions have been made. The VH of scFv-B1.3.9 belongs to the VH-I subgroup having highest homology to germline segment DP-4. Three mutations have been identified. The changes from $Met^{2} \rightarrow Val^{2}$ and $Met^{89} \rightarrow Val^{89}$ are conservative. Valine is preferentially found in the other germline segments of the VH-I subgroup and can therefore be judged to be a non-problematic change. The third mutation, however, is a critical nonsense mutation leading to an amber stop codon at position 64 ($Gln^{64} \rightarrow amber^{64}$). This explains why the expression of soluble scFv was not successful while strong reactivity was observed for the phage-displayed scFv-B1.3.9 (Figure 2B). The phage-displayed scFv is expressed in *E. coli* TG1, which is a suppressor strain to allow the expression of a fusion-protein between the pIII and the scFv. TG1 can introduce glutamine at amber stop codons, thus restoring the authentic germline residue at position H64. In contrast, *E. coli* strain HB2151 used for production of soluble scFv is a non-suppressor

strain. As a result, no functional soluble form of scFv-B1.3.9 is produced in this strain.

In order to overcome the problem of the nonsense mutation introduced at position H64 of scFv-B1.3.9, preventing the expression of a soluble form of the scFv, it was converted to the designated germline sequence using SOE-PCR (see Methods). The corrected clone was sequenced to confirm the introduction of the Gln^{64} coding sequence (data not shown) and this new clone was designated scFv-B1.3.9^{c}.

Characterization of B1.3.9^{c} and B5.2.14 – Nine ampicillin resistant colonies were selected for production of soluble scFv-B1.3.9^{c} (Figure 4). All clones expressed functional scFvs that bound to $EtxB_1$ showing that the acquired nonsense mutation was successfully and properly corrected. We then went on to analyze the binding specificity of scFv-B1.3.9^{c} by comparing the binding against $EtxB_1$ and directly coated $EtxB_5$. As was previously observed for the phage-displayed B1.3.9 (Figure 2A), the soluble scFv-B1.3.9^{c} exhibited equivalent binding activity against both $EtxB_1$ and directly coated $EtxB_5$ suggesting it recognizes a shared epitope. However scFv-B1.3.9^{c} was shown not to bind to $EtxB_5$ captured to G_{M1}-ganglioside (Figure 4) suggesting the epitope becomes inaccessible when the complex is formed.

We then used a recently described, well-characterized conformation specific monoclonal antibody for comparison to B5.2.14 (Chung *et al.*, 2006). LDS16 is a neotope-specific monoclonal antibody that binds to directly coated as well as to G_{M1}-ganglioside captured $EtxB_5$ and does not recognize $EtxB_1$. As in our previous study we looked at the specificity of the antibodies by concentration dependent inhibition assays (Figure 5). As we described previously LDS16 binding to coated $EtxB_5$ was inhibited in the presence of soluble $EtxB_5$. However, while B5.2.14 binding was partially inhibited, this only reached a maximum level of 10% (Figure 5A). As expected, LDS16 binding to G_{M1} captured $EtxB_5$ was not inhibited by $EtxB_1$ and there was no binding of B5.2.14 to G_{M1} captured $EtxB_5$ (Figure 5B). Lastly, there was no inhibition of either LDS16 or B5.2.14

binding to $EtxB_5$ coated plates by $EtxB_1$ produced by boiling $EtxB_5$ (Figure 5C), while there was a marked contrast in the results obtained by using boiled and reduced $EtxB_5$ (Figure 5D). Here, $EtxB_1$ (DTT) markedly inhibited the binding of B5.2.14 to $EtxB_5$ coated plates while, as shown previously, LDS16 binding was unaffected. This was confirmed using western blotting, which showed that B5.2.14 only reacted with DTT reduced $EtxB_5$, and not with boiled $EtxB_5$ (Figure 5E). These results serve to illustrate the rather subtle but distinctive differences of the binding specificities between these two recombinant antibodies.

DISCUSSION

Here we have reported the successful isolation of scFvs against EtxB by phage display. As in previous studies with conventional mAbs (Chung *et al.*, 2006) we have set out to define individual scFvs that can differentiate between different forms of EtxB.

We and others have previously used a combination of ELISA and SDS-PAGE to study the kinetics of both EtxB and CtxB assembly (Ruddock *et al.*, 1995). In later experiments we used a combination of these techniques and tryptophane fluorescent spectroscopy to elucidate a kinetic model of how toxin assembly *in vitro* may take place (Lesieur *et al.*, 2002). It was shown that assembly of $CtxB_5$ occurs via ordered formation of oligomeric species and that they can equally go through two alternative pathways to form the fully assembled pentamer. In addition, other experiments investigating A/B subunit assembly have suggested that holotoxin formation requires the A-subunit to interact with a B-subunit assembly intermediate rather than with fully assembled $CtxB_5$ (Hirst, 1995).

Our studies using conventional mAbs have identified epitopes potentially important for investigating pentameric subunit assembly but these have limitations for use in studying assembly *in vivo* (Chung *et al.*, 2006). Recombinant single-chain Fv antibodies potentially offer a great

advantage in this respect. Other studies using monoclonal scFvs against (*H. pylori*) urease (Reiche *et al*., 2002) and hepatitis B virus surface antigen (HBsAg) (Zhang *et al.*, 2006) have highlighted the advantage of this approach. In the first instance anti-urease antibodies derived from *H. pylori* infected patients have helped to define important antigenic epitopes involved with disease recovery (Reiche *et al*., 2002) and in the second instance anti-HBsAg scFvs are being used to develop strategies to block viral entry (Zhang *et al*., 2006). In addition these anti-HBsAg scFvs fused with interferon can be used as a reagent in the therapy of chronic hepatitis B (Zhang *et al*., 2006). These newly prepared anti-EtxB scFvs open up considerable scope for extending earlier studies by potentially enabling the interaction of antibodies with toxin assembly intermediates to be carried out both *in vitro* and *in vivo*.

Selection was performed against two different forms of EtxB, the heat dissociated disassembled monomeric form $EtxB_1$ and the assembled pentameric form $EtxB_5$. After two to three rounds of panning monoclonal phage-ELISA showed that phagemid clones were selected that exhibited binding specificity to $EtxB_1$ or $EtxB_5$ (Figure 2). Further characterization of individual clones allowed us to focus on one phagemid with specificity for $EtxB_1$ (scFv-B1.3.9) and one with specificity for $EtxB_5$ (scFv-B5.2.14) (Table 1, Figure 2). We should note that although no isolated scFvs showed specificity for $EtxB_1$ without cross-reactivity to directly coated $EtxB_5$ we do have some preliminary evidence (data not shown) that such scFvs may be present in the library.

Since both B5.2.14 and $B1.3.9^c$ do not bind to G_{M1}-ganglioside captured $EtxB_5$ it could be hypothesized that they recognize an epitope that overlaps with the G_{M1}-ganglioside binding site or an epitope that is located at the bottom surface of the pentameric EtxB. The surface potential of both $EtxB_5$ and $CtxB_5$ in this region is highly basic to facilitate binding to the negatively charged cell surface (Figure 6B). Thus, it is rational to expect that an antibody binding in this region would have

an antigen-binding site with a negative surface potential. However, inspection of the amino-acid composition of the CDRs (Figure 3) shows a relatively high preponderance of basic residues for both B1.3.9^{c} and B5.2.14. Theoretical calculations of the Fv iso-electric points yielded 9.8 for B1.3.9^{c} and 9.6 for B5.2.14. To further support this notion we generated homology models for both scFvs to specifically look for the charge distribution in the paratope.

Both paratopes exhibit highly basic surfaces (Figures 6C and D) that make it unlikely that either B1.3.9^{c} or B5.2.14 would recognize an epitope located at the bottom side of pentameric EtxB although this cannot be excluded. Interestingly, the peptides identified by Marcel *et al.* (in this issue) were also highly basic, suggesting that similar binding regions were targeted by both approaches. Moreover, binding of the phage-displayed peptides to $EtxB_5$ was not inhibited by soluble G_{M1}-ganglioside and soluble $EtxB_5$ bound to phages dotted onto nitrocellulose. Thus steric hindrance offers no complete or satisfying explanation for the observed lack of binding towards G_{M1}-ganglioside captured $EtxB_5$. The specificity of B1.3.9^{c} is, in fact, strongly reminiscent of the conventional mAb LDS47 against an N-terminal region of $EtxB_1$ (Figure 6A) that we previously described which also bound to directly coated $EtxB_5$ (Amin *et al.*, 1995).

The fine specificity of B5.2.14 was investigated using competition ELISA assays with the conventional mAb LDS16 as a comparison (Figure 5). This gave an intriguing result. Firstly, soluble $EtxB_5$ inhibition of binding to directly coated $EtxB_5$ was only marginal (Figure 5A). We can think of only two possible explanations for this 10% maximal inhibition: a) the existence of different conformational states of the epitope and b) the presence of disassembled intermediates. Since disassembled intermediates would only constitute a small fraction of the total protein because of the high intrinsic stability of the pentameric form we believe the existence of different conformational states of the epitope to be more likely. We have previously hypothesized that

a conformational change occurs in the protein upon binding to a solid surface exposing an epitope not normally accessible in the fully folded conformation (Lesieur *et al*., 2002). Similar conclusions have been drawn from studies with the β2 subunit of *E. coli* tryptophan synthase (Friguet *et al*., 1984). Secondly, although, as we showed earlier (Figure 2B), there was no binding in ELISA of scFv-B5.2.14 to denatured (boiled) $EtxB_1$, in Figure 5D we clearly show that DTT reduced/denatured $EtxB_1$ strongly inhibits binding to $EtxB_5$. These results were confirmed by western blotting, which not only gave an appropriate band (Mr = 12,000) for the denatured/boiled EtxB but also gave a faint band (Mr = 43,000) consistent with $EtxB_5$ (Figure 5E). Thus, this is almost certainly a conformation dependent epitope (cryptotope) probably of a folding intermediate structure (Figure 6A) and could be an ideal target for studying pentamer formation *in situ*. It would be interesting to repeat these inhibition experiments with $B1.3.9^c$ to look at its finer specificity.

In conclusion, this paper reports the generation of two scFvs with differential binding specificities that may provide useful molecular probes for studying EtxB pentamer assembly. The availability of such reagents opens up key areas for the development of new therapeutics that can block toxin formation *in situ* and thus be used for the treatment of diarrhoeal diseases caused by *E. coli* and *V. cholera*.

ACKNOWLEDGEMENTS

We would like to thank Dr. Andrew Griffiths for providing the Griffin.1 human scFv library (MRC, Cambridge, UK). Work on delineating models of CtxB assembly (Lesieur *et al.*) and initial studies on screening the Griffin.1 library was kindly funded by the BBSRC (7/C10265)

REFERENCES

Aman, A. T., Fraser, S., Merritt, E. A., Rodigherio, C., Kenny, M., Ahn, M., Hol, W. G., Williams, N. A.,Lencer, W. I., and Hirst, T. R. (2001) *Proc Natl Acad Sci U S A* **98**(15), 8536-8541

Amin, T., and Hirst, T. R. (1994) *Protein Expr Purif* **5**(2), 198-204

Amin, T., Larkins, A., James, R. F., and Hirst, T. R. (1995) *J Biol Chem* **270**(34), 20143-20150

Bost, K. L., and McGhee, J. R. (1996) *J Infect Dis* **173**(3), 627-635

Chothia, C., Lesk, A. M., Gherardi, E., Tomlinson, I. M., Walter, G., Marks, J. D., Llewelyn, M. B., and Winter, G. (1992) *J Mol Biol* **227**(3), 799-817

Chung, W. Y., Carter, R., Hardy, T., Sack, M., Hirst, T. R., and James, R. F. (2006) *J Biol Chem* **281**(51), 39465-39470

Echeverria, P., Seriwatana, J., Taylor, D. N., Yanggratoke, S., and Tirapat, C. (1985) *Am J Trop Med Hyg* **34**(3), 547-554

Fishman, P. H., Moss, J., and Osborne, J. C., Jr. (1978) *Biochemistry* **17**(4), 711-716

Fishman, P. H., Pacuszka, T., Hom, B., and Moss, J. (1980) *J Biol Chem* **255**(16), 7657-7664

Fraser, S. A., de Haan, L., Hearn, A. R., Bone, H. K., Salmond, R. J., Rivett, A. J., Williams, N. A., and Hirst, T. R. (2003) *Infect Immun* **71**(3), 1527-1537

Friguet, B., Djavadi-Ohaniance, L., and Goldberg, M. E. (1984) *Mol Immunol* **21**(7), 673-677

Gough, K. C., Li, Y., Vaughan, T. J., Williams, A. J., Cockburn, W., and Whitelam, G. C. (1999) *J Immunol Methods* **228**(1-2), 97-108

Griffiths, A. D., Williams, S. C., Hartley, O., Tomlinson, I. M., Waterhouse, P., Crosby, W. L., Kontermann, R. E., Jones, P. T., Low, N. M., Allison, T. J., and et al. (1994) *Embo J* **13**(14), 3245-3260

Guex, N., and Peitsch, M. C. (1997) *Electrophoresis* **18**(15), 2714-2723

Hirst, T. R. (1995) Bacterial Toxins and Virulence Factors in Disease. In: Moss, J., Vaughan, M., Iglewski, B., and Tu, A.T. (ed). Handbook of Natural Toxins, Marcel Dekker Inc., New York

Holmgren, J., Lonnroth, I., Mansson, J., and Svennerholm, L. (1975) Proc Natl Acad Sci U S A 72(7), 2520-2524

Kuziemko, G. M., Stroh, M., and Stevens, R. C. (1996) Biochemistry 35(20), 6375-6384

Lesieur, C., Cliff, M. J., Carter, R., James, R. F., Clarke, A. R., and Hirst, T. R. (2002) J Biol Chem 277(19), 16697-16704

Luross, J. A., Heaton, T., Hirst, T. R., Day, M. J., and Williams, N. A. (2002) Arthritis Rheum 46(6), 1671-1682

Merritt, E. A., Sarfaty, S., Jobling, M. G., Chang, T., Holmes, R. K., Hirst, T. R., and Hol, W. G. (1997) Protein Sci 6(7), 1516-1528

Nissim, A., Hoogenboom, H. R., Tomlinson, I. M., Flynn, G., Midgley, C., Lane, D., and Winter, G. (1994) Embo J 13(3), 692-698

Reiche, N., Jung, A., Brabletz, T., Vater, T., Kirchner, T., and Faller, G. (2002) Infect Immun 70(8), 4158-4164

Ruddock, L. W., Ruston, S. P., Kelly, S. M., Price, N. C., Freedman, R. B., and Hirst, T. R. (1995) J Biol Chem 270(50), 29953-29958

Shevach, E. M. (2000) Annu Rev Immunol 18, 423-449

Sixma, T. K., Pronk, S. E., Kalk, K. H., van Zanten, B. A., Berghuis, A. M., and Hol, W. G. (1992) Nature 355(6360), 561-564

Sobel, D. O., Yankelevich, B., Goyal, D., Nelson, D., and Mazumder, A. (1998) Diabetes 47(2), 186-191

Takahashi, I., Marinaro, M., Kiyono, H., Jackson, R. J., Nakagawa, I., Fujihashi, K., Hamada, S. Clements, J. D.,

Williams, N. A., Stasiuk, L. M., Nashar, T. O., Richards, C. M., Lang, A. K., Day, M. J., and Hirst, T. R. (1997)

Proc Natl Acad Sci U S A 94(10), 5290-5295

Tomlinson, I. M., Walter, G., Marks, J. D., Llewelyn, M. B., and Winter, G. (1992) J Mol Biol 227(3), 776-798

Truitt, R. L., Hanke, C., Radke, J., Mueller, R., and Barbieri, J. T. (1998) Infect Immun 66(4), 1299-1308

Turnbull, W. B., Precious, B. L., and Homans, S. W. (2004) J Am Chem Soc 126(4), 1047-1054

Weiner, H. L. (1997) Immunol Today 18(7), 335-343

Williams, N. A., Hirst, T. R., and Nashar, T. O. (1999) Immunol Today 20(2), 95-101

Wilson, A. D., Bailey, M., Williams, N. A., and Stokes, C. R. (1991) Eur J Immunol 21(10), 2333-2339

Yamamoto, T., Gojobori, T., and Yokota, T. (1987) J Bacteriol 169(3), 1352-1357

Zhang, J. L., Gou, J. J., Zhang, Z. Y., Jing, Y. X., Zhang, L., Guo, R., Yan, P., Cheng, N. L., Niu, B., and Xie, J. (2006) Hepatobiliary Pancreat Dis Int 5(2), 237-241

FIGURE LEGENDS

Figure 1. Enrichment of polyclonal phages panned against EtxB monomers and pentamers. The polyclonal phages after the 1st, 2nd and 3rd round of panning were tested for reactivity against monomeric and pentameric EtxB by direct phage-ELISA. Enrichment of scFvs against the pentamer was more efficient and the polyclonal phages exhibited only low reactivity against monomeric (boiled) EtxB. Phages selected for binding to monomeric EtxB, on the other hand, were enriched less efficiently and showed significant cross-reactivity against pentameric EtxB.

Figure 2. Binding specificities of monoclonal phages. (**A**) Several phages were selected for a large-scale phage preparation and their binding reactivities against different EtxB forms were analysed by ELISA. (**B**) Soluble scFvs were produced for 4 monoclonal phages and were analysed by ELISA.

Figure 3. Sequence analysis of scFv-B1.3.9 and scFv-B5.2.14. Sequences were aligned to the human germline segments reported in the V-BASE directory (http://vbase.mrc-cpe.cam.ac.uk/index.php). CDRs were assigned according to Cothia and are shown in bold. DP-L3, DP-L16, DP-14 and DP-4 are the designations of the germline sequences that most closely resemble those of the two scFvs and deviations are indicated. The insertion sites where the random sequences have been introduced are indicated by a gap.

Figure 4. ELISA for soluble scFv-B1.3.9^{c}. Nine ampicillin-resistant colonies were picked and used for small scale expression of soluble scFv-B1.3.9^{c}. Culture supernatants were analysed against monomeric (boiled) EtxB, directly coated $EtxB_5$ and G_{M1}-captured $EtxB_5$ by ELISA.

Figure 5. Inhibition of the binding of B5.2.14 and LDS16 to different forms of soluble EtxB. (**A**) Plates were coated directly with $EtxB_5$ (B5c) and probed with B5.2.14 or LDS16 and binding was inhibited by increasing concentrations of free $EtxB_5$. (**B**) Plates were coated directly with $EtxB_5$ (B5c) and boiled EtxB was used for competition. (**C**) Plates were coated directly with $EtxB_5$ (B5c) and boiled and DTT treated EtxB was used as inhibitor. (**D**) Recognition of different forms of EtxB by scFv-B5.2.14 in Western-blot. Lane 1, Boiled $EtxB_1$; Lane 2, $EtxB_5$; Lane 3, Boiled and reduced (DTT) $EtxB_1$. The single headed arrow denotes the positions of the monomeric form and the double headed arrow of the pentameric form.

Figure 6. 3D-visualization of molecular features of the pentameric B-subunit and scFv-B1.3.9 and scFv-B5.2.14. **(A)** Graphical illustration of antibody epitopes mapped onto proposed dimeric EtxB folding intermediates. The second EtxB protomer (cyan) is shown in two alternate conformations. In the folded form Pro^{93} (single headed arrow) is in the *cis* state and Cys^9 and Cys^{86} form a disulfide-bridge. The β-strand number 6 is shown in grey. In proposed partially folded dimers the cysteines are reduced and Pro^{93} is in the *trans* configuration (double headed arrow). Assembly can only proceed after isomerisation of Pro^{93} and disulfide-bridge formation. MAb LDS102 recognizes to the C-terminal end of $EtxB_1$ and partially inhibits re-assembly (Chung et al 2006). The epitope of mAb LDS47 has been mapped to the N-terminal residues involving Cys^9 (red and orange), but binding is independent of the redox-state. In contrast, scFv-B5.2.14 recognizes a different form and only binds to heat-denatured and reduced EtxB. ScFv-B1.3.9 recognizes a cryptotope that is not accessible in the assembled pentamer but becomes exposed after heat-denaturation. Similarly to LDS47 but contrary to scFv-B5.2.14, reduction of the disulfide-bridge is not a required for binding. **(B)** Visualisation of the surface potentials of $EtxB_5$. The bottom side is highly basic to facilitate binding to the negatively charged cell surface receptor. The top

surface is characterised by a cluster of acidic residues comprising Asp^{22}, Glu^{79} and the C-terminus. Both scFv-B1.3.9 **(C)** and scFv-B5.2.14 **(D)** have high theoretical iso-electric points of 9.8 and 9.6 respectively. The surfaces potentials were mapped onto homology-modelled structures and are viewed from the top, looking down at the paratope. The antigen-binding site of scFvB1.3.9 is highly positively charged, suggesting binding to a negatively charged region.

Table 1: Characterization of selected scFvs

	Clone	OD 450nm	Scaled up phage prep	As soluble scFv
Monomer (B1)	3.1	0.4	No reactivity	-
	3.6	0.3	No reactivity	-
	3.9	1.0	+ve for monomer (1.0)	No scFv found in C, P or S
Pentamer (B5)	2.6	0.2	Slight reactivity (0.1)	-
	2.11	1.0	Positive for Pentamer	scFv found in C only
	2.14	1.0	Positive for Pentamer	scFv found in C, P and S
	2.15	0	No reactivity	-

C - cytoplasmic fraction; P - periplasmic fraction; S - culture supernatant

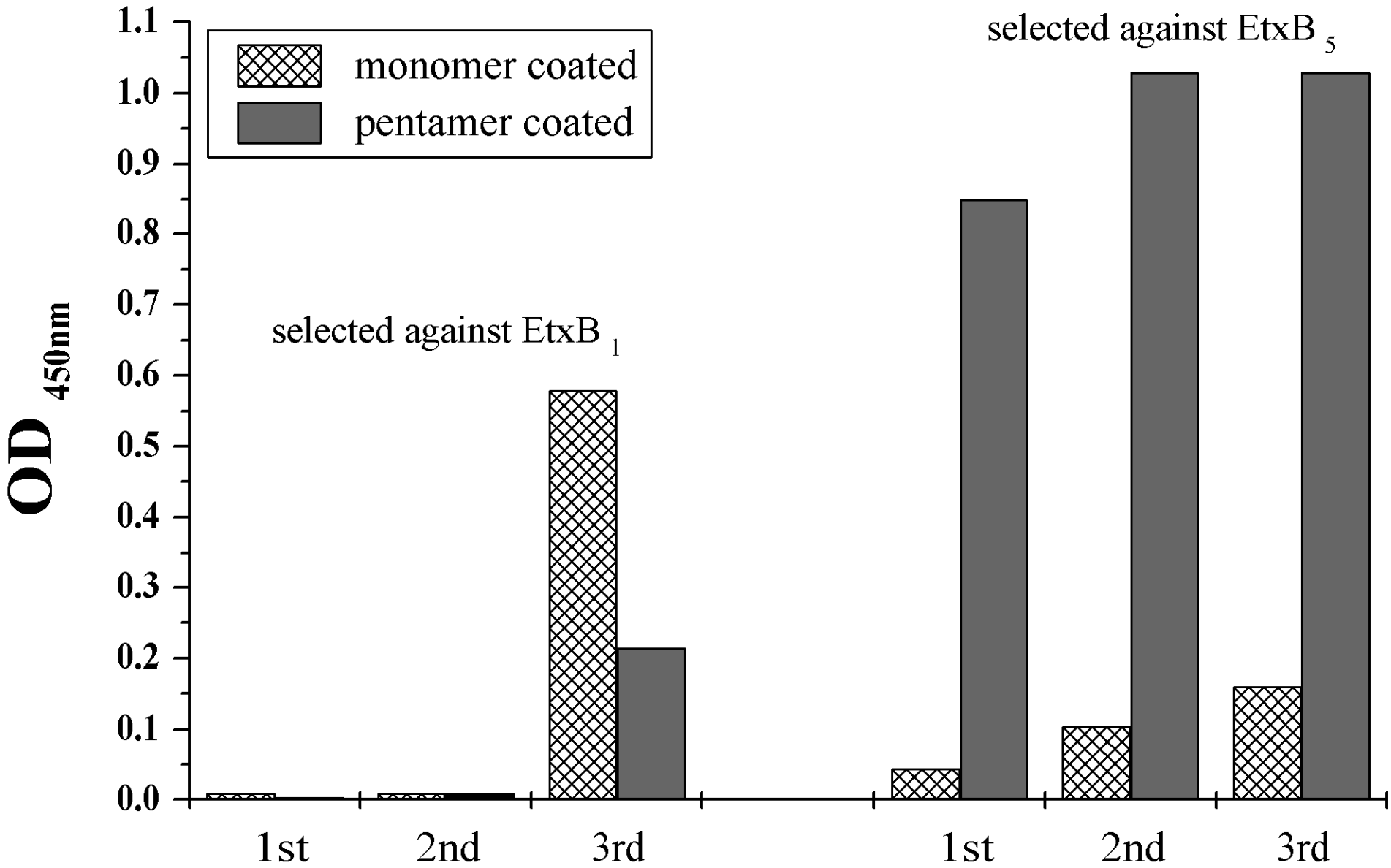
monomer coated
pentamer coated
selected against EtxB 1
selected against EtxB 5
OD 450nm
1.1
1.0
0.9
0.8
0.7
0.6
0.5
0.4
0.3
0.2
0.1
0.0
1st
2nd
3rd
1st
2nd
3rd

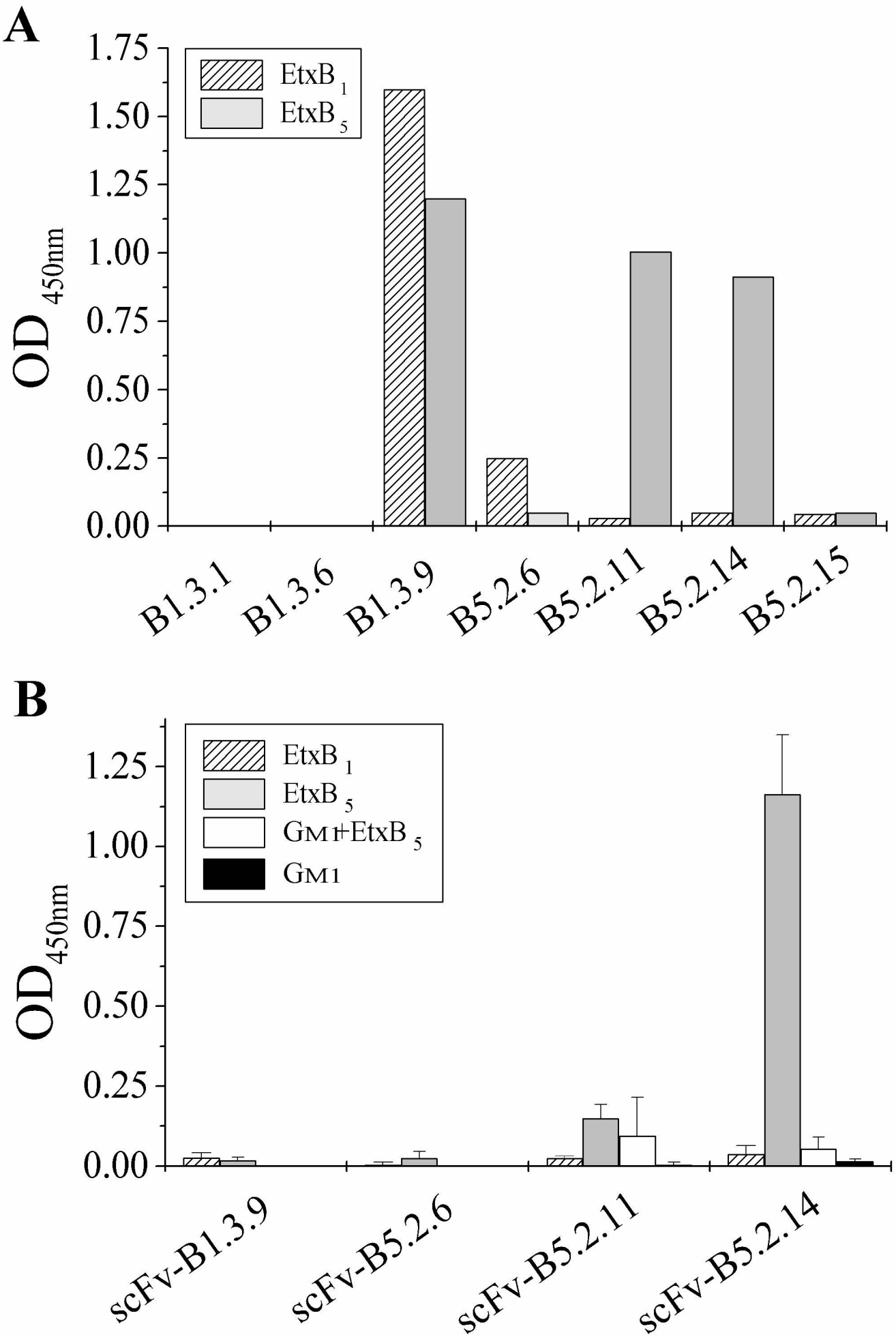
A
1.75
1.50
1.25
1.00
0.75
0.50
0.25
0.00
OD450nm
EtxB1
EtxB5
B1.3.1
B1.3.6
B1.3.9
B5.2.6
B5.2.11
B5.2.14
B5.2.15
B
1.25
1.00
0.75
0.50
0.25
0.00
OD450nm
EtxB1
EtxB5
GM1+EtxB5
GM1
scFv-B1.3.9
scFv-B5.2.6
scFv-B5.2.11
scFv-B5.2.14


light-chains
CDR-L1
CDR-L2
DP-L3
B5.2.14 QSVLTQPPSASGTPGQRVTISCSGSSSNIGSNYVYWYQQLPGTAPKLLIYRNNQRPS
B1.3.9 SSELIQDPAVSVALGQTVRITCQGDSL--RSYYASWYQQKPGQAPVLVIYGKNNRPS
DP-L16 T
CDR-L3
DP-L3 G
B5.2.14 GVPDRFSGSKSGTSASLAISGLRSEDEADYYCAAWDDSLSA LV FGGGTKLTVL
B1.3.9 GIPDRFSGSSSGNTASLTITGAQAEDEADYYCNSRDSSGTV -- FGGGTKLTVL
DP-L16 NH
heavy-chains
CDR-H1
CDR-H2
DP-14
B5.2.14 QVQLVQSGAEVKKPGASVKVSCKASGYTFTSYGISWVRQAPGQGLEWMGWISAYNGNTNYAQ
B1.3.9 QVQLVQSGAEVKKTGSSVKVSCKASGYTFTYRYLHWVRQAPGQALEWMGWITPFNGNTNYAQ
DP-4 M
CDR-H3
DP-14 W
B5.2.14 KLQGRVTMTTDTSTSTAYMELRSLRSDDTAVYYCAR GRPPRPLRPSQV LGQGTLVTVSS
B1.3.9 KF*DRVTITRDRSMSTAYMELSSLRSEDTAVYYCAR GTLKRI----RN WGQGTLVTVSS
DP-4 Q M

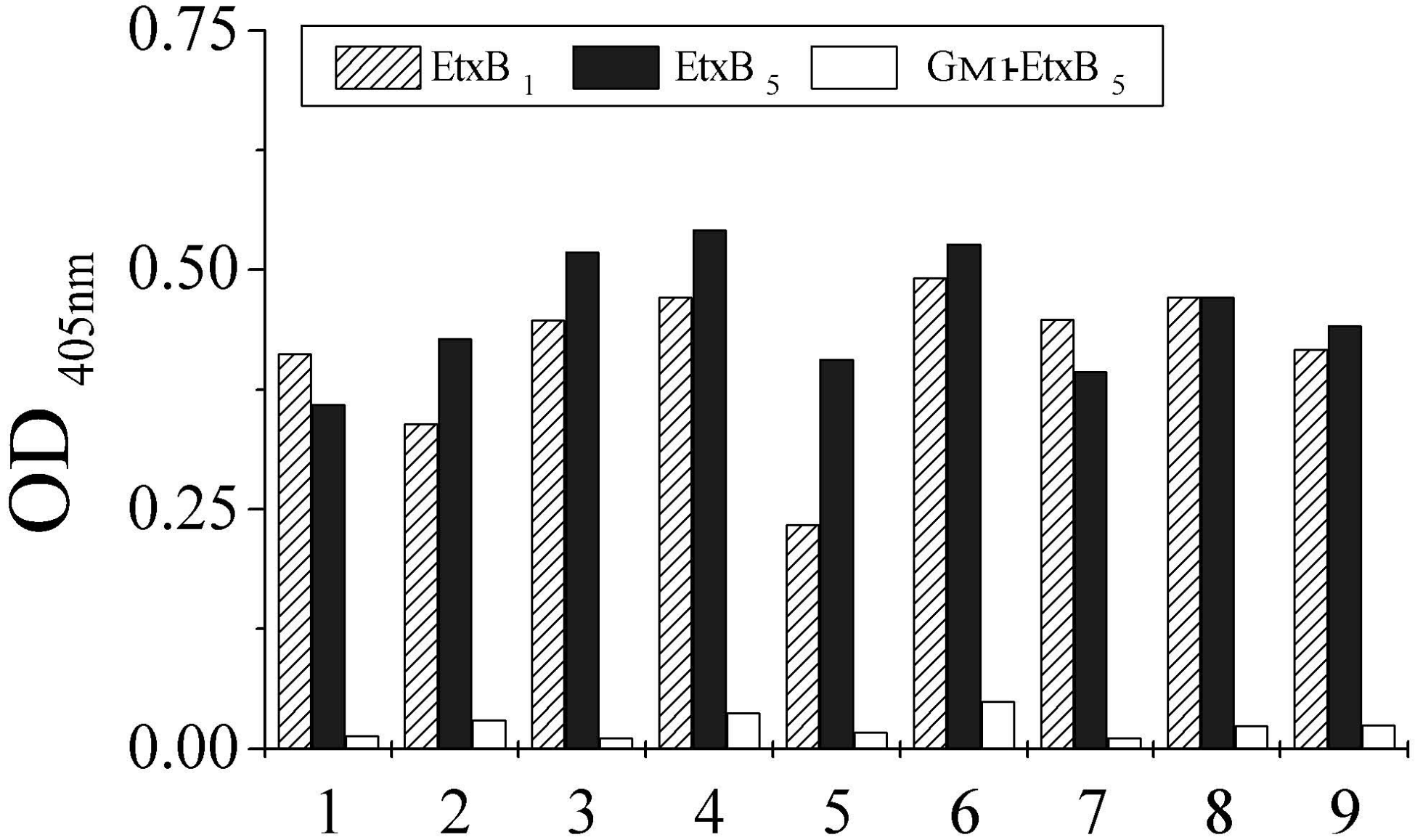
EtxB 1
EtxB 5
GM1-EtxB 5
OD 405nm
0.75
0.50
0.25
0.00
1
2
3
4
5
6
7
8
9

(A)

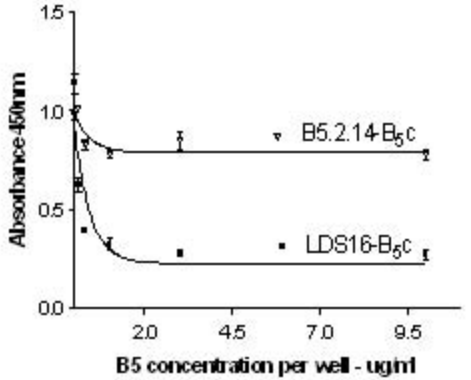
1.5
1.0
0.5
0.0
Absorbance-450nm
B5.2.14-B5c
LDS16-B5c
2.0
4.5
7.0
9.5
B5 concentration per well - ug/ml

(B)

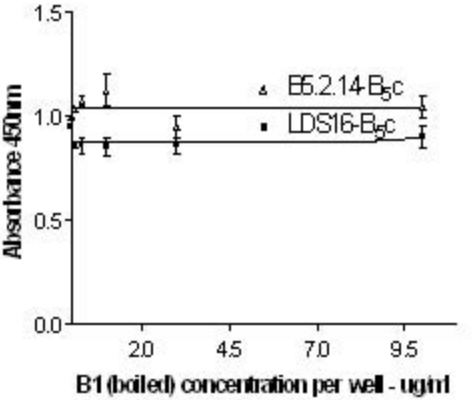
1.5
1.0
0.5
0.0
Absorbance-450nm
B5.2.14-B5c
LDS16-B5c
2.0
4.5
7.0
9.5
B1 (boiled) concentration per well - ug/ml

(C)

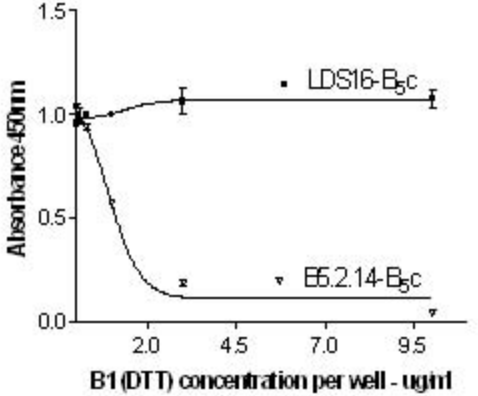
1.5
1.0
0.5
0.0
Absorbance-450nm
LDS16-B5c
B5.2.14-B5c
2.0
4.5
7.0
9.5
B1 (DTT) concentration per well - ug/ml

(D)

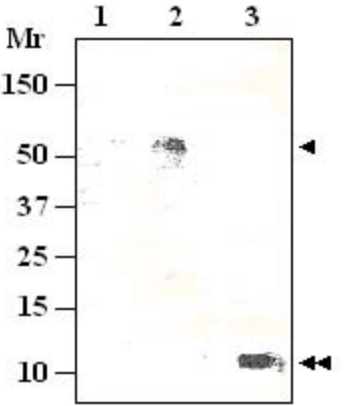
1
2
3
Mr
150
50
37
25
15
10

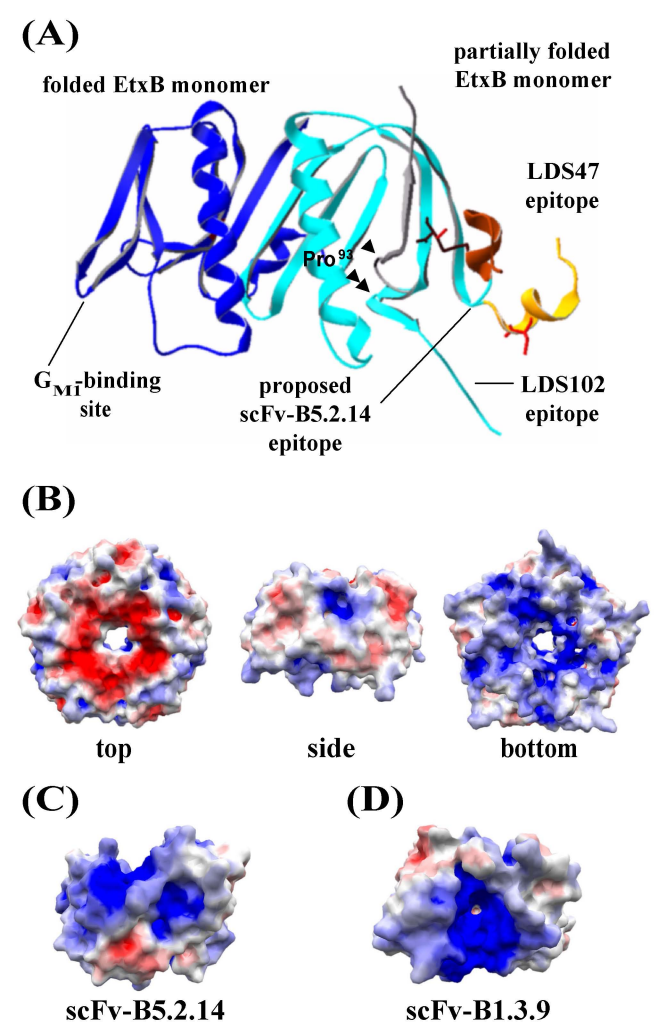
(A)
folded EtxB monomer
partially folded EtxB monomer
LDS47 epitope
Pro 93
G M1 binding site
proposed scFv-B5.2.14 epitope
LDS102 epitope
(B)
top
side
bottom
(C)
(D)
scFv-B5.2.14
scFv-B1.3.9